J Paleolimnol (2010) 44:645–666
DOI 10.1007/s10933-010-9445-1

ORIGINAL PAPER

Use of fine-scale stratigraphy and chemostratigraphy to evaluate conditions of deposition and preservation of a Triassic *Lagerstätte*, south-central Virginia

C. M. Liutkus · J. S. Beard · N. C. Fraser · P. C. Ragland

Received: 13 March 2009 / Accepted: 19 May 2010 / Published online: 5 June 2010

Abstract The rich, fossiliferous Triassic sediments exposed in the Virginia Solite Quarry include a 34-mm-thick "insect layer" that is notable for detailed preservation of soft-bodied invertebrate and vertebrate remains. We describe this unique *Konservat-Lagerstätte* and use sedimentologic and geochemical analyses to interpret the environmental conditions necessary to preserve such delicate fossils. This work is among the first attempts to apply detailed geochemical/stratigraphic analysis to the study of *Lagerstätten* and we report on a 332-mm-thick section that includes the insect layer and the rocks immediately below and above it. Our analysis successfully constrains various aspects of the depositional and diagenetic history of the *Lagerstätte* and permits a detailed analysis of changing conditions prior to, during, and after deposition. Geochemical and sedimentologic analyses of the insect layer and surrounding lithologies reveal a change from siliciclastic-dominated layers (Unit 1) to dolomite-siliciclastic laminites above (Unit 2 and the insect layer), separated by a boundary dolostone layer that is traceable for over 200 m. We interpret this sedimentary shift as the initial stages in the transgression of a shallow, saline, alkaline rift-basin lake over lake margin deposits. The absence of bioturbation by plants and benthic organisms, as well as a lack of predation on the insects, is not explained by significant water depth, but is instead more reasonably considered a result of the chemistry of the water at the lake margin, affected by groundwater seeps, which provided F-, Mg-, and Ca-rich fluids. Although the initial conditions of preservation are remarkable, it is equally impressive that the fossils survived extensive diagenesis, e.g. dissolution of quartz and coarsening of dolomite.

Keywords Rift basin · Lacustrine · Newark Supergroup · Insects · Danville-Dan River Basin

P. C. Ragland—deceased.

C. M. Liutkus (✉)
Department of Geology, Appalachian State University, Boone, NC 28607, USA
e-mail: liutkuscm@appstate.edu

J. S. Beard · N. C. Fraser · P. C. Ragland
Virginia Museum of Natural History, Martinsville, VA 24112, USA

N. C. Fraser
National Museums Scotland, Edinburgh EH1 1JF, UK

Introduction

Konservat-Lagerstätten—strata that preserve soft parts and soft-bodied forms with exceptional fossil preservation—provide a unique picture of the entire spectrum of life in a fossil ecosystem. They are among the most important paleontologic sites on

Earth, and include the Burgess Shale, Solnhofen Limestone, Green River Formation, Barstow Formation, and others. Understanding the conditions under which these and other fossil deposits form is crucial in gaining a detailed re-creation of past ecologic systems (Park and Downing 2001; Gierlowski-Kordesch and Park 2004; Fürsich et al. 2007). The research herein aims to describe and understand the depositional and diagenetic environment of a Triassic *Lagerstätte* within the Danville-Dan River Basin of south-central Virginia through detailed stratigraphic, paleontologic, and chemical analyses. By delineating the conditions necessary for exquisite preservation of insect fossils at this site, we illustrate a depositional model that can be applied to other rift basin sites that will aid in the location and interpretation of new non-marine *Lagerstätten*. The conclusions presented here are also important for the ongoing study of these Triassic rift-basin depositional environments because the data appear to indicate a strikingly different depositional environment (shallow littoral) than has been suggested previously for dark fine-grained, laminated lacustrine sediments.

Geologic and geographic setting

The Dan River-Danville basin is part of the Mesozoic rift system in eastern North America that formed during the breakup of the supercontinent Pangaea during the Triassic (Olsen et al. 1989; Schlische 2003). The basin is an elongate half-graben with a southeast-dipping border fault system, the Chatham fault zone. The basin is ~170 km long and its width ranges from 3 to 15 km (Fig. 1a). The 4,000 m of tilted basin fill (Dan River Group) immediately overlie (unconformably) Proterozoic and Paleozoic igneous rocks, gneisses, and amphibolites, e.g. the Smith River Allochthon (Horton and McConnell 1991). Additionally, Paleozoic sedimentary rocks (including barite-bearing crystalline limestone) are found to the north/northwest of the site (Watson and Grasty 1915). The Virginia Solite Quarry is situated in the middle of the basin where it straddles the North Carolina-Virginia state line at Cascade, VA (Fig. 1a). The Solite sedimentary rocks are considered to be among the richest and most productive Triassic terrestrial sequences in the world (Fraser et al. 1996). The diversity of insects is particularly significant, but plants and vertebrates are also well represented.

The Solite Quarry comprises three separate quarries, designated A, B, and C (Fraser and Grimaldi 2003; Fig. 1b). Together, they expose several hundred meters of the largely lacustrine upper member of the Cow Branch Formation (Meyertons 1963; Olsen et al. 1991; Kent and Olsen 1997). Although previously considered Carnian (Olsen et al. 1989), following the work of Muttoni et al. (2004), a Norian age is now preferred. The Cow Branch Formation represents the lacustrine, middle member of the Dan River Group, which begins and ends with fluvially-derived siliciclastics of the Pine Hall and Stoneville Formations, respectively (Olsen et al. 1991). Within the Cow Branch Formation, bedded lacustrine shales,

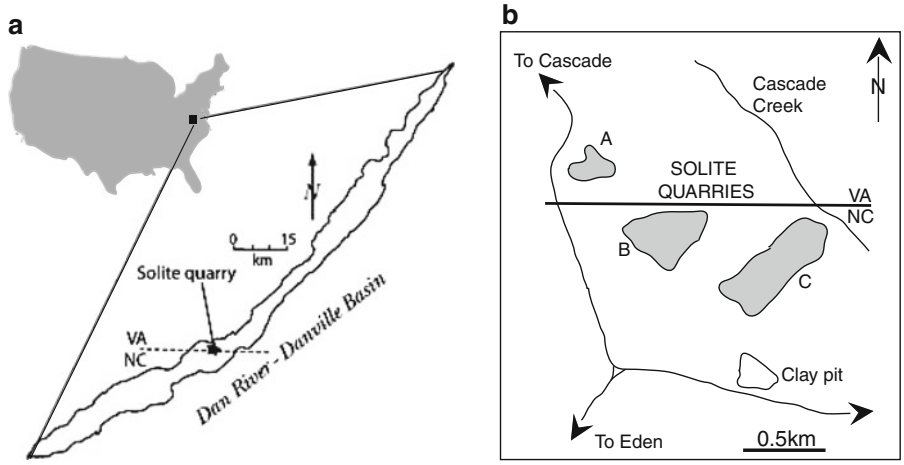

Fig. 1 **a** Location of the Solite quarry within the Danville-Dan River Basin. **b** Map showing the location of Quarries *A*, *B*, and *C* within the Solite Quarry's boundary. Modified from Fraser and Grimaldi (2003)

mudstones, and sandstones preserve Van Houten cyclicity, thought to reflect changes in lake level and precipitation due to Milankovitch orbital changes that affect solar radiation.

In various Newark Basin exposures, Olsen and Johansson (1994) suggest that these cycles reflect conditions ranging from complete desiccation to a lake 200 m or more in depth. Olsen (1986) divided each Van Houten cycle into three divisions based upon lake depth: Division 1, red to purple root-marked sandstones produced by lake transgression; Division 2, black, laminated mudrocks with fish remains representing a lake highstand interval; and Division 3, gray to red bioturbated siliciclastics developed during lake regression and a subsequent low stand. At the Solite Quarry, seventeen repetitive sedimentary sequences, Van Houten cycles, are exposed in Quarry B and each is $\sim$10 m thick (Olsen 1986).

Olsen and Johansson (1994) noted that there is an unusually fossiliferous cycle near the top of Quarry B, designated cycle 2 in Fig. 2 by Olsen (1979), where soft-bodied insects are preserved in the basal portion of a Division 2 sequence. They interpret these particular layers as reflecting deposits of a deep, stratified lake, possibly the deepest lake sediments in the cycle. The lack of bioturbation and exceptional preservation of vertebrate and invertebrate fossils supposedly reflect an anoxic bottom environment (Olsen and Johansson 1994). This fossiliferous section was termed the "insect layer" by Fraser et al. (1996). Recent work (Fraser and Grimaldi 2003; Grimaldi et al. 2004, 2005) confirmed that the preservation of insects and vertebrate soft parts is largely confined to the laminated lower 3 cm of Division 2 in cycle 2, i.e., the insect layer (Fig. 2), although there are other, more restricted insect-producing units elsewhere in the quarries.

The insects are sparsely distributed throughout the "insect layer," although there are some dense accumulations of belostomatids, particularly nymphs, with up to 50 or more individuals on a 150 cm^2 area of a bedding plane. By comparison with other notable Triassic insect localities, such as the Molteno Formation of South Africa (Anderson et al. 1996) or the Grès à Voltzia of eastern France (Gall 1971), the Solite accumulations are rich and, to date, over 4,000 specimens have been collected. Aquatic forms, including larvae of dipterans, dominate the assemblage, but it is also notable for a diversity of terrestrial groups including coleopterans (beetles), thysanopterans (thrips), blattoids (cockroaches), and many dipterans (true flies) (Fraser et al. 1996; Blagoderov et al. 2007; Fig. 3). The insect bed is also characterized by dense accumulations of conchostracan valves that sometimes obscure details of the insects. A variety of macrophyte plant fossils, including fern, cycad, and conifer leaf fragments, are preserved throughout the insect bed, but there is no evidence of bioturbation such as root traces, burrows, etc. A number of specimens of the small aquatic tetrapod *Tanytrachelos ahynis* were also recovered from the insect layer. These are invariably fully articulated and preserve elements of soft tissue including skin and myotome muscle blocks (Fraser et al. 1996). Fish are exceptionally rare and only a single specimen was taken from the insect layer during the intensive collecting of the past 12 years.

Methods

A newly excavated, unweathered, and continuous 332-mm-thick section was sampled in 1998 from the north side of Quarry B (Fig. 2). The base of the section lies within a carbonaceous siltstone immediately subjacent to the insect layer (Fig. 2). The top of the measured section is the base of a zone of intense local syn- to post-depositional deformation that appears to be confined to a single bed or series of beds <10 cm thick. Nevertheless, it is obvious that the continuity of the section above this layer, particularly at the scale of our study, is compromised by the deformation. Samples for this study were removed as oriented blocks. For the purpose of description and chemical analysis, we defined fourteen named blocks based on natural breaks along bedding planes (Table 1).

Each block contains many beds, some of which are microlaminated. It is important to note that the individual blocks do not necessarily define individual stratigraphic units. However, taken together, the fourteen blocks define three units with distinctive chemistry, sedimentology, and stratigraphy separated by clear boundary layers (Table 1).

A portion of each of the fourteen blocks was crushed in a stainless steel mill and analyzed for major and trace elements by standard X-ray fluorescence (XRF) and inductively coupled plasma (ICP) techniques. Total carbon, sulfur and CO_2 were

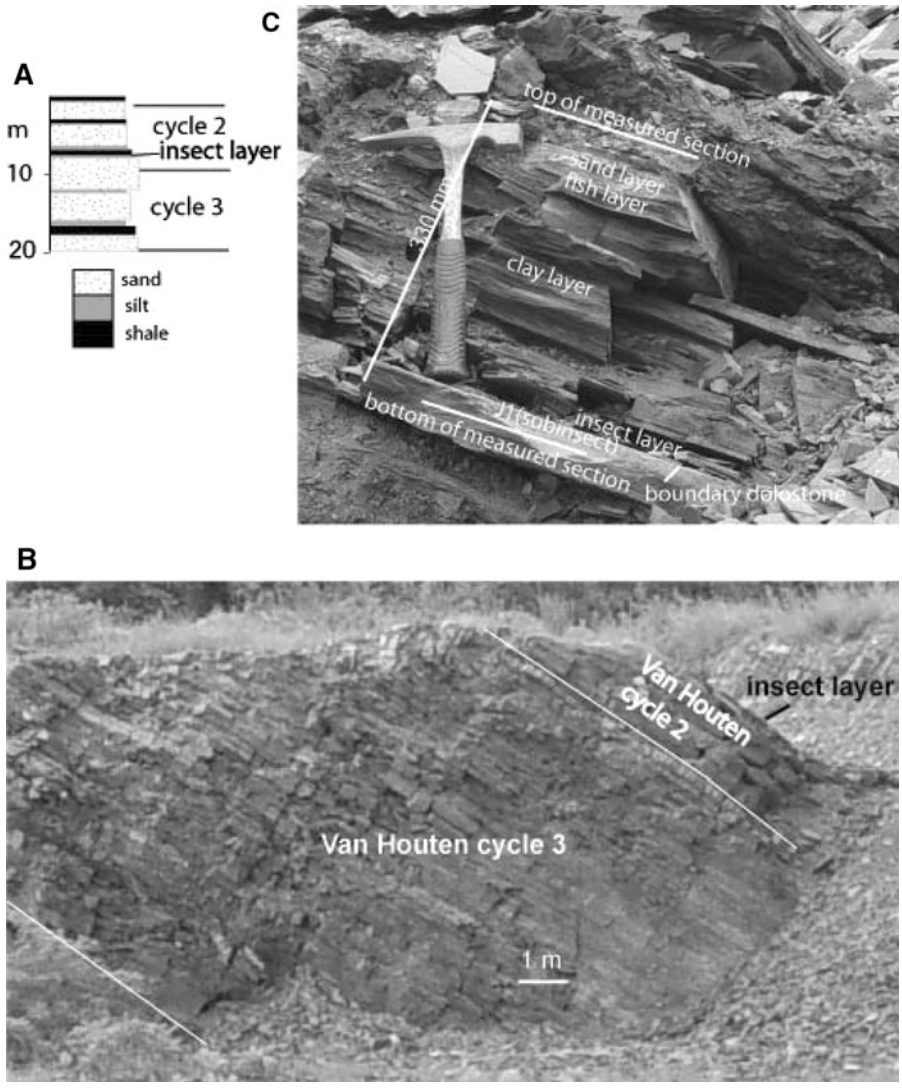

Fig. 2 **a** Stratigraphic setting of the insect layer. The column (modified after Olsen et al. 1989) shows the top 20+ m of the quarry section and Van Houten cycles 2 and 3. The insect layer lies within cycle 2. The base of cycle 1 is at the top of the section. **b** Exposure of cycle 3 and the base of cycle 2 in the west wall of Quarry B. The insect layer and layers immediately above have been excavated. **c** The 332-mm measured section in situ. Labeled layers described in Table 1

determined by a combination of wet chemical and infrared spectrometry techniques at ActLabs, Ltd. Organic carbon values were determined by an additional total carbon analysis after extraction of carbonate from the sample.

A continuous series of oriented, polished thin sections was prepared from the blocks. Dolomite rhombs were analyzed by electron microprobe, with a core and rim analysis collected approximately every 1 mm throughout the 332-mm section. The entire measured section was analyzed by broad-beam electron microprobe (rastered beam, 0.5 × 0.5 mm) for major elements, including S and F. These analyses yielded low totals (35–45%) due to distortion of the X-ray detection region, consequent to broad-beam analysis. Values were normalized to major element analyses obtained by XRF from the blocks, and the totals rose to between 70 and 90%, with low totals corresponding to dolomite-rich, i.e. CO_2-rich, areas. We consider the microprobe analyses to be semi-quantitative and use them as a tool to describe general compositional and stratigraphic trends.

Results

Field and mesoscopic features

The 332-mm section consists of microlaminated carbonaceous, dolomitic black shales, with a few

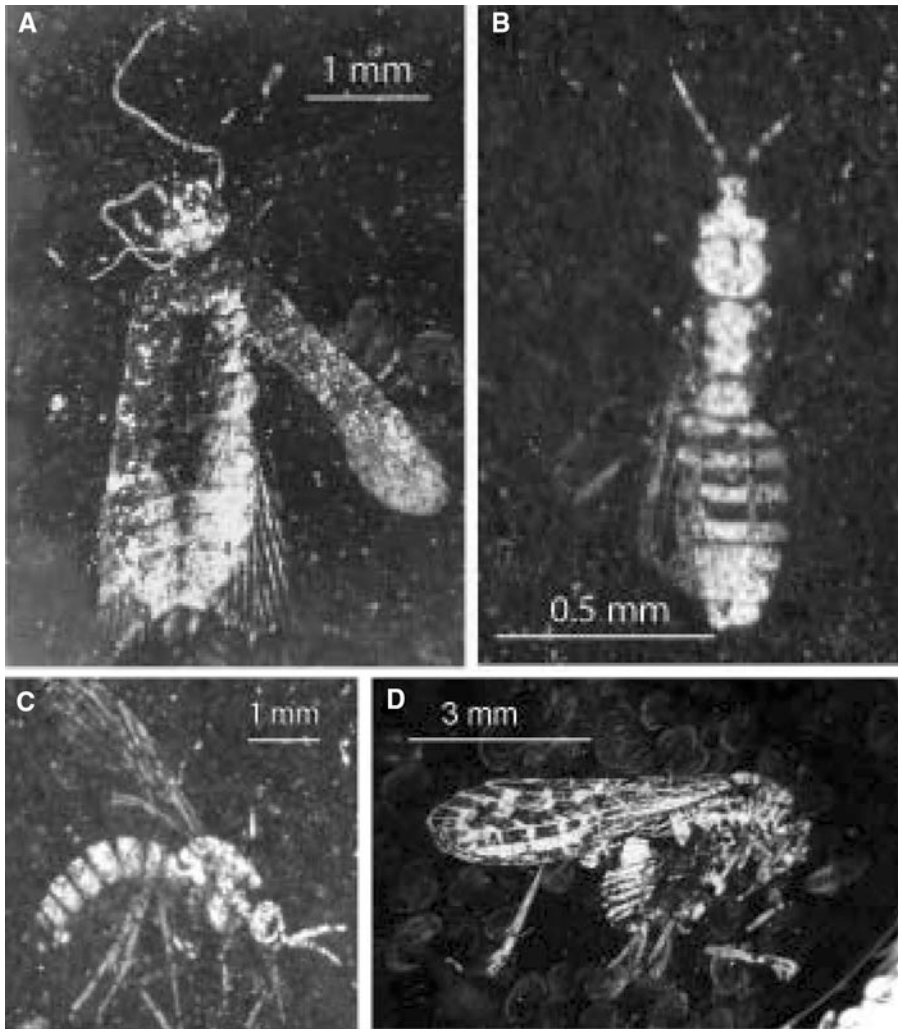

Fig. 3 Triassic insects from the insect layer, Solite Quarry. **a** Cockroach. **b** Crane fly. **c** Thrips. **d** Elcanid orthopteran

interbedded sandy layers near the top of the section (units D1 and D2; Fig. 4). There is no evidence of bioturbation. The section is heavily jointed and cut by numerous, laterally discontinuous mesoscopic and microscopic normal faults typical of tensional stress. Ackermann et al. (2003) provide a detailed description of the tectonic features exposed at the Solite Quarry.

Petrography and lithotypes

Sand- to silt-sized siliciclastic (mostly feldspar) and carbonate (dolomite) grains occur in discrete laminae that range in thickness from one mm to several cm. Most laminae are <0.5 cm thick and many of these are discontinuous or lensoidal. Grains can also occur as discontinuous trains or isolated grains in laminated and dolomitic sediments.

Dolomite occurs in all samples and rock types. Optically- and chemically-zoned dolomite occurs as anhedra and as subhedral to euhedral rhombs, 0.02–0.10 mm in maximum dimension (Fig. 4a). Fine-grained rocks with clay-sized particles, are laminated, with discontinuous laminae defined by (1) shaley partings, (2) gradational variations in the ratio of dolomite to clay, and (3) changes in the color of the clay fraction. Most carbonaceous material is amorphous, interstitial, and opaque, even at the thin edge

Table 1 Layer and unit characteristics

Layer name for chemical analysis	Thickness (mm)	Special layer descriptors	Layer characteristics	Unit	Unit characteristics
C	38		Top of unit truncated by shear zone. *Tanytrachelos* abundant in top 3 mm. Low S in top 30 mm	3	Carbonaceous, carbonate and clastic rich. Locally contains thin (1–10 mm) graded sandstone beds. Poorly laminated. Locally rich in coprolites and plant debris. Interpreted as deeper water. High sulfur except at top of layer "C", locally high P, U, HREE. Anoxic black shale
D1	23	Sandstone layer	Single, medium-grained sand bed	3	
D2	64	Fish layer	High P, U, HREE abundant fish fossils and coprolites	3	
Etop	11			3	
Ebot	19			3	
F1top	5			3	
F1bot	18	Claystone layer	Almost pure clay shale	2, Boundary between Units 2 and 3	>90% clay
F2top	14			2	Clay and carbonate rich, little silt or sand, laminated, relatively poor in C and S. Dysoxic "gray shale"
F2bot	27			2	
Gtop	16			2	
Gbot	18			2	
H	17		Includes conchostracan layer	2	
I	17			2	
J1	28	Insect layer	Insect and invertebrate fossils. Fish rare and small	2	
Boundary dolostone	2	Boundary dolostone	Nearly pure dolostone with mudcracks	At basal boundary of insect layer	>90% ferroan dolomite, hiatus at top
J2	15	Sub-insect layer	Carbonaceous siltstone	1	Carbonaceous, carbonate-poor, siltstone with weak and discontinuous layering

Not all boundaries between layers represent a significant change in lithology (e.g. Ebot to Etop) and instead represent natural breaks between layers in outcrop

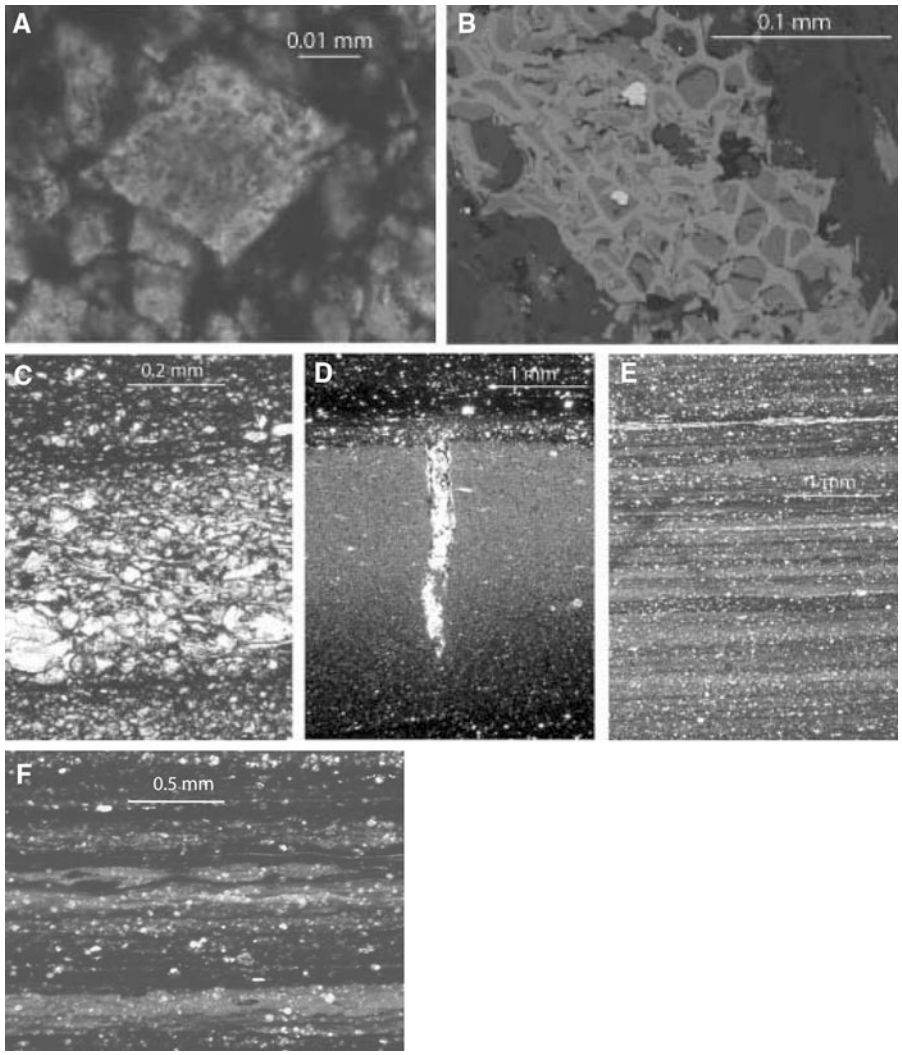

Fig. 4 Photomicrographs, plane polarized light unless noted. Scale refers to distance along base of photograph. Block designation follows Table 1. **a** Dolomite rhomb. Core appears darker because of numerous inclusions. Block Etop. **b** Carbonaceous plant fossil showing high reflectivity and cell structure. Highly reflective grains are pyrite. Reflected light, block D1. **c** Graded silt bed within carbonaceous dolostone, block Etop. **d** Boundary dolostone (Table 1; Fig. 3). Note wedge-shaped, downward-pointing fracture. Below layer is carbonaceous siltstone of unit 1, above is the insect layer at the base of unit 2 (Table 1). Note difference in color. Also note that the dolomite layer becomes less carbonaceous upward. **e** Laminated structure, insect layer, block J1. Colorless grains are mostly dolomite

of polished sections. However, coal-like fragments of plant material are common throughout the section, especially in the coarser-grained lithologies. In reflected light, these fragments are highly reflective and strongly anisotropic, bireflectant, and pleochroic and may exhibit cellular structures (Fig. 4b). Discrete, rounded to irregular carbonaceous nodules that contain well-developed euhedra of apatite are interpreted as phosphatized coprolites or gastric ejecta (P. Olsen, pers. commun. 1994).

Siltstones and sandstones

Black, carbonaceous sandstones and siltstones occur as well sorted, commonly graded beds <1–30 mm thick (Fig. 4c). Individual clasts are angular and dominated by feldspar (mostly albite), but micas (biotite and muscovite) are also common. Despite its abundance in local basement rocks, quartz is absent in all but a few samples. Where found, quartz appears to be partially replaced by dolomite.

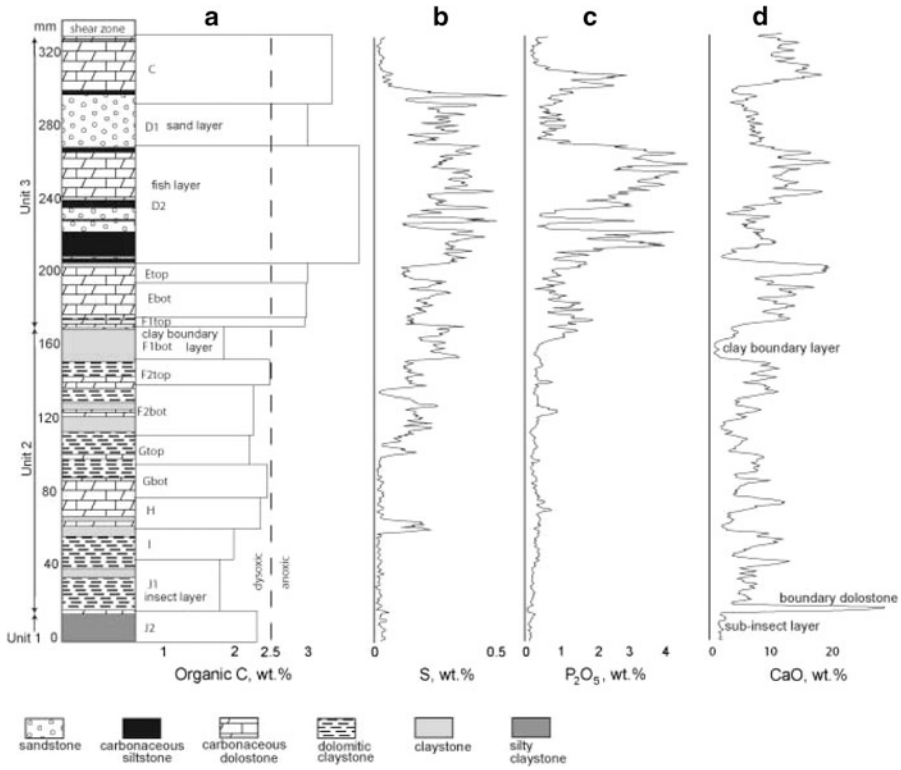

Fig. 5 Stratigraphy and chemostratigraphy. Layer and block terminology as in Table 1. Stratigraphic column based on thin section petrography. See text. **a** Organic carbon. Dysoxic-anoxic boundary for marine black shales after Algeo and Maynard (2004) shown for reference only. **b** Total S. **c** P_2O_5. **d** CaO. **a** is based on whole rock analyses of blocks. **b**, **c**, and **d** are 3-point moving averages of continuous broad-beam electron microprobe analyses with a rastered 0.5-mm spot size

Dolomite is always an important constituent of the sandy/silty layers in the measured section. It occurs as euhedral rhombs, distorted or broken rhombs, and polycrystalline aggregates, has micas deformed around it, and locally shows size grading similar to that shown by other clast types. Other constituents of the clastic layers include amphibole, ilmenite, and (organic) carbonaceous material. The latter is mostly an opaque and largely unresolvable interstitial material, but includes some large plant fragments and coprolites.

Claystones

Rocks described as claystone or dolomitic claystone (Fig. 5) contain clay-sized particles and exhibit strongly pleochroic, translucent, golden-reddish-brown to dark chocolate-brown laminae. Under plane-polarized light, entire layers show simultaneous and striking color change upon stage rotation. Under crossed nicols, extinction is also simultaneous. No vestige of individual clay particles is discernible under the light microscope, either in transmitted or reflected light. The color of the clay reflects organic content and gradations of color within layers are common. The darkest brown clay can grade almost imperceptibly into opaque, carbonaceous material.

Most claystones contain 10–30% dolomite, but individual laminae may have dolomite contents as high as 80%. Rocks with >30% dolomite, whose clay fraction is largely opaque, are termed carbonaceous dolostones. This designation is also applied to the boundary dolostone that separates the insect bed from the underlying silty claystone. This unique unit consists of >80% very fine-grained microspar (<0.02 mm) dolomite.

Within the J1 block (the insect layer), carbonate laminites are prevalent (Fig. 6a). Couplets of microsparry dolomite and carbonaceous clay (which exhibits a wavy surface) are abundant. Additionally, peloid-like blebs are rarely evident within the dolomitic layers (Fig. 6b). These elongate features are aligned with respect to each other, consist of dolomitic microspar, and appear to meld together to form composite, wavy, dolomitic laminae reminiscent of microbial mats. Clay drapes are noticeable above these wavy laminae, and

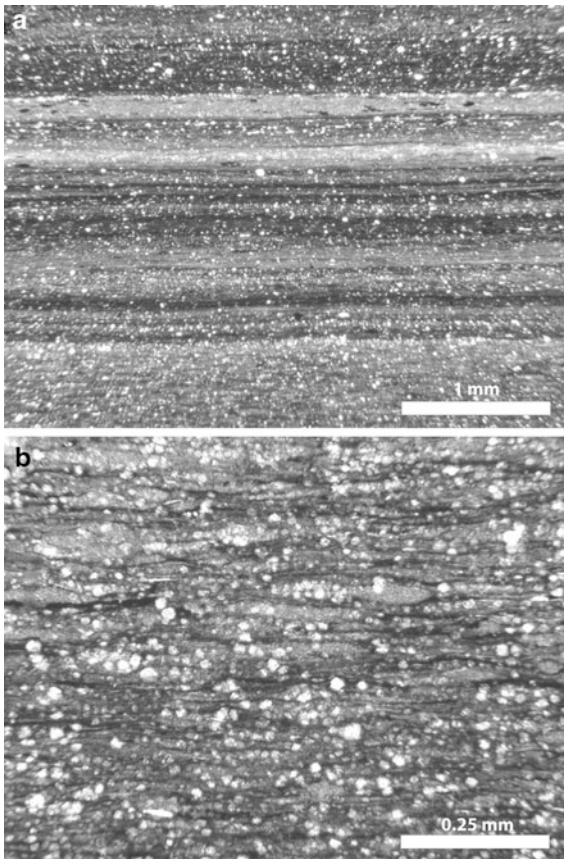

Fig. 6 **a** Carbonate laminites found in the J1 block. Microsparry dolomite alternates with carbonaceous clay. **b** Peloid-shaped features in J1bot sediments

soft sediment deformation beneath these layers is rare, but evident.

Stratigraphy

The measured section can be subdivided into three major units with several distinctive layers within those units (Table 1; Fig. 5).

Unit 1

The basal unit (Unit 1 = Block J2) consists of micaceous, silty claystone that lies beneath the insect layer (J1). Fine-scale layering in Unit 1 is poorly developed and defined by discontinuous lenses of sand or silt-sized silicates. Unit 1 is unique in its combination of weak layering, high clay content, high siliciclastic content, and low carbonate content.

Boundary dolostone

A thin, carbonaceous dolomite layer ranging in thickness from 0 to 3 mm, and called the "boundary dolostone," marks the top of Unit 1 (Fig. 4d). The top of this unique horizon, which was not included in the chemical analyses of either J1 or J2, defines the base of the insect layer. Although disrupted on the scale of cm, the boundary dolostone is recognizable over a lateral distance of 210 m. The layer consists of microsparry dolostone that is carbonaceous at the base, with decreasing organic carbon content towards the top. The layer is broken at irregular intervals and exhibits numerous downward-pointing wedge-shaped cracks (2–3 mm deep, 0.5 mm wide) that are filled with a crystalline (non-clastic) silicate mineral (Fig. 4d). The dolostone surrounding these cracks is not deformed upward and the material infilling the cracks appears to remain resistant and extends above the top of the boundary dolostone layer, suggesting that the layer has been eroded and the more-resistant infill remains as a cast of the former crack. No siliciclastic detritus is found in the cracks.

Unit 2

Unit 2 consists of the insect layer itself and the next seven blocks, J1 through the bottom of F1. This part of the measured section is characterized by abundant claystone and dolomitic claystone (75% of the measured section), and a paucity of siliciclastic material coarser than clay, with <1% silt distributed as thin layers and lenses. The unit is finely, but discontinuously, laminated throughout, with layering defined by variations in carbonate content, variations in clay color, and partings between dolomite-rich laminae (Fig. 4e). Intraclasts of the boundary dolostone are found within the base of Unit 2.

Claystone boundary layer

The top of Unit 2 is marked by an 18-mm-thick, carbonate-poor, laminated claystone, the "clay boundary layer" in block F1bot. This is the finest-grain-size unit in the measured section and is markedly deficient in dolomite compared to the layers below and above it. A thin siltstone at the top of the clay boundary layer marks the base of Unit 3.

Unit 3

The top 160 mm of the section, comprised of blocks F1top through C, contains abundant carbonaceous siltstones, sandstones, and carbonaceous dolostones with a noticeable lack of clay-sized material. Siltstone and sandstone make up >40% of Unit 3 and claystone lithologies <5%. This unit includes several graded sand beds >5 mm thick, including one that is 30 mm thick, the "sand layer" in block D1. Silty or sandy layers that are irregularly intercalated with massive carbonaceous dolostone define most of the fine-scale layering in Unit 3. Block D2 in Unit 3 is the thickest in the measured section and consists of interbedded dolostone, siltstone, and sandstone. It is rich in plant material, coprolites, and fish remains and is termed the "fish layer."

Geochemistry and chemostratigraphy

Geochemical features

CaO correlates strongly with CO_2 and can be taken as a chemical proxy for carbonate in the measured section (Figs. 5, 7a). The negative correlation between CaO and Al_2O_3 reflects the summative relationship between the carbonate and siliciclastic components in the Solite section (Fig. 7b). Alkalis largely reside in the siliciclastic component. Regardless of CaO, i.e., carbonate content, Si/Al

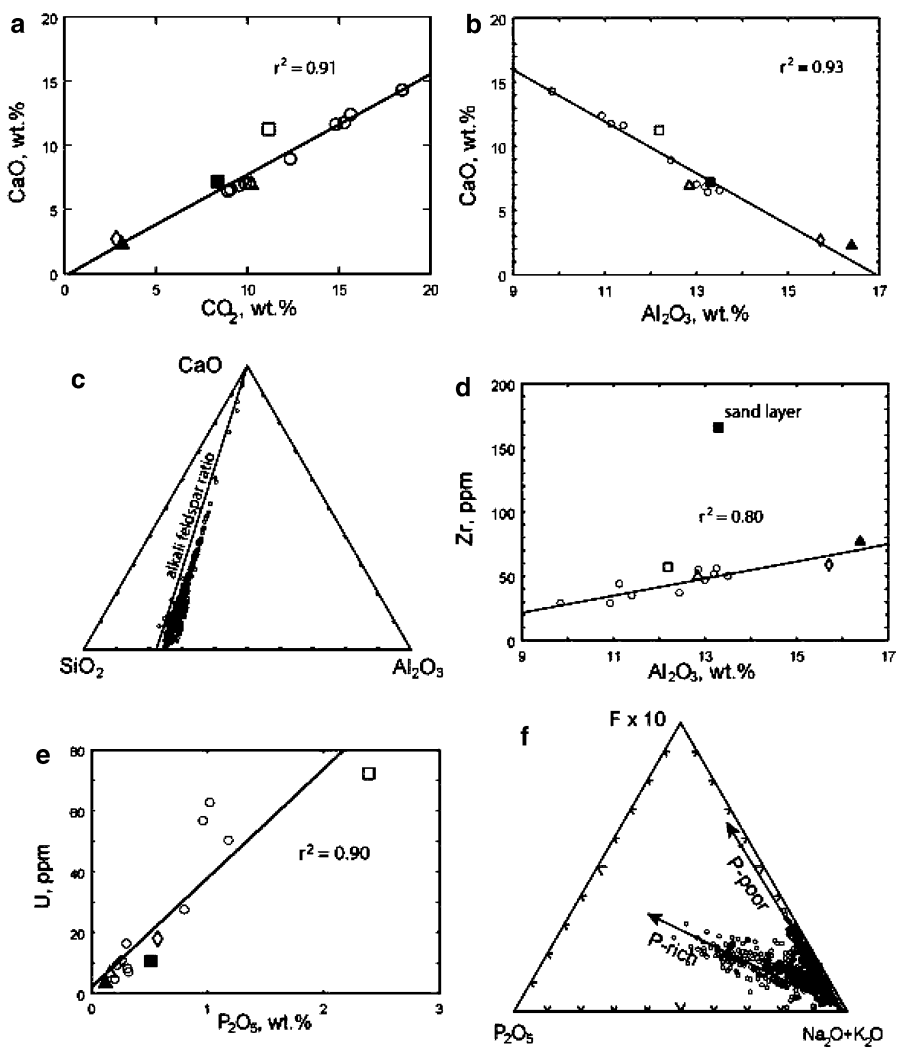

Fig. 7 Whole rock analyses. **a** CO_2 vs. CaO. On this and subsequent figures, r^2 is linear correlation coefficient squared. **b** Al_2O_3 vs. CaO. **c** SiO_2–CaO–Al_2O_3. Note that most analyses are more aluminous than alkali feldspar. **d** Al_2O_3 vs. Zr. **e** P_2O_5 vs. U. **f** P_2O_5-F*10-$Na_2O + K_2O$. Note dual enrichment trends for **f**. **a**, **b**, **d**, and **e** are whole-rock analyses of blocks; **c** and **f** represent broad-beam microprobe analyses with a spot size of 0.5 mm. Key to block analyses: *filled triangle*, subinsect layer (block J1; Unit 1); *open triangle*, insect layer (block J1), *open diamond*, clay boundary layer (block F1bot); *open square*, fish layer (block D2); *filled square*, sand layer (block D1). All other blocks are represented by *open circles*

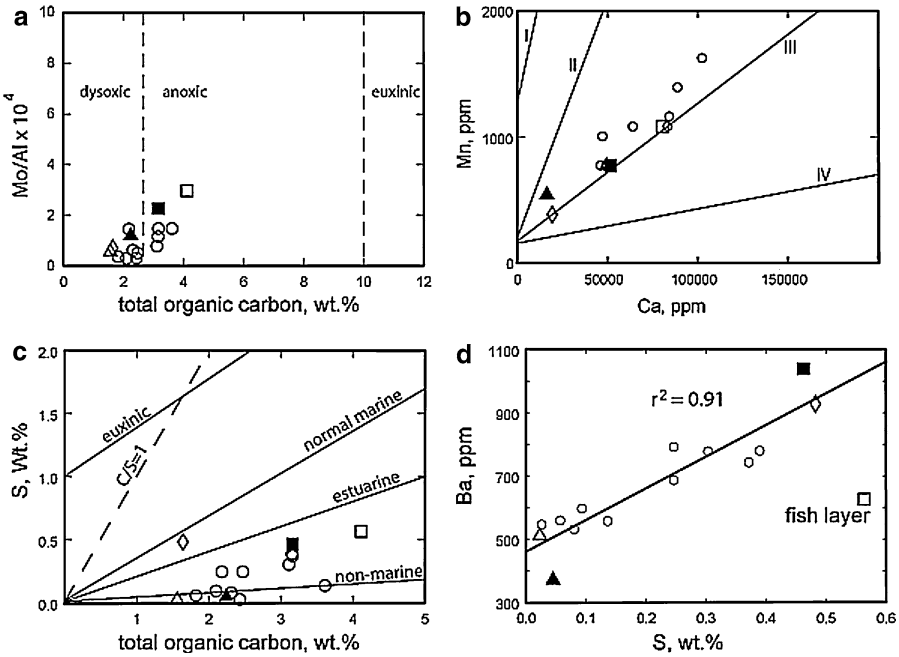

Fig. 8 **a** Organic C vs. Mo/Al. Fields following Algeo and Maynard (2004) are for marine shales and are shown for reference only. **b** Ca vs. Mn. Discriminate for calcic shales following Quinby-Hunt and Wilde (1996). Lines I and II are largely oxic, lines III and IV are largely anoxic. **c** Organic carbon vs. sulfur. Lines after Heggie and Skyring (2005) (estuarine). Other lines after Berner and Raiswell (1984) and Leventhal (1995). **d** S vs. Ba. Symbols defined as in Fig. 7

(and Si/alkali) ratios remain nearly constant (Fig. 7c). The low Si/Al ratio of the siliciclastic component indicates that clay minerals rather than quartz or feldspars dominate (Fig. 7c). Zr, as well as Nb and Ti, correlate positively with Al_2O_3, indicating their presence within the siliciclastic component (Fig. 7d). The thickest sand layer (D1, Table 1) contains excess Zr, suggesting that this element resides largely in the coarser fraction, presumably as zircon.

Several blocks from the upper layers of the measured section contain substantial (1–3%) P_2O_5. Heavy Rare Earth Elements (HREE), and U increase with phosphate (Fig. 7e). Phosphatic rocks also have elevated concentrations of fluorine, presumably contained in fluor-apatite. We note that elevated F is also found in some P-poor samples, most importantly from the insect layer (Fig. 7f).

Organic C concentrations in the measured section range as high as 4 wt% and samples straddle the divide between dysoxic and anoxic marine shales (Fig. 8a). Transition metals correlate weakly with organic carbon, but never approach the levels found in euxinic marine shales (Fig. 8a; Algeo and Maynard 2004). Ca and Mn concentrations also suggest an environment that is transitional between dysoxic and anoxic (Fig. 8b; Quinby-Hunt and Wilde 1996). These metals serve as direct independent measures of oxidation and support the inferences made on the basis of TOC. High C/S in the measured section is typical of freshwater to brackish water sediments (Fig. 8c; Berner and Raiswell 1984; Heggie and Skyring 2005). Although pyrite is found in most samples, a strong correlation between S and Ba suggests that at least some of the S is in the form of sulfate, e.g., barite (Fig. 8d).

Chemostratigraphy

Overall, the measured section is characterized by striking upsection increases in organic C, S, and phosphate (Fig. 5). The insect layer (J1) has the lowest organic C and S content of any sample in the measured section (Fig. 5). Organic carbon is >2.5% in all Unit 3 samples and <2.5% in all Unit 1 and 2 samples. P_2O_5 is <0.5% below the clay boundary layer (F1bot) and reaches values of >3% in parts of Unit 3, especially the fish layer (D2). S begins to increase towards the top of Unit 2 and increases through most of Unit 3 before dropping at the top of the section (block C). The C/S ratio has high values (>30) in Unit 1 and most of Unit 2, but drops locally to <5 in the upper part of Unit 2 and Unit 3. CaO, a carbonate proxy, is low in Unit 1, increases dramatically in the boundary dolostone, and then stabilizes at a high concentration throughout the measured

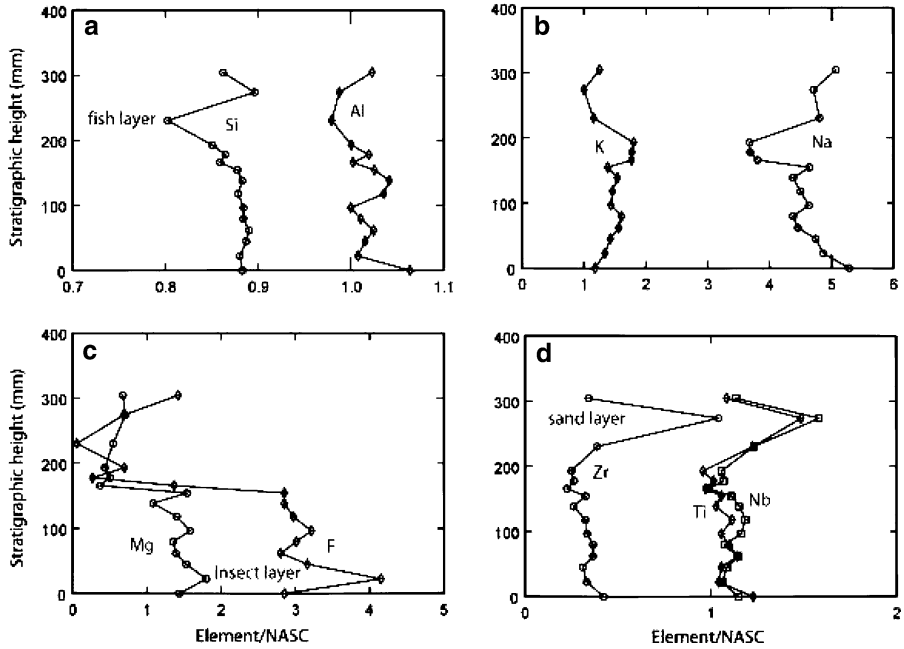

Fig. 9 Stratigraphy vs. siliciclastic chemistry. Siliciclastic chemistry is calculated by subtracting carbonate and phosphate fractions from the whole-rock analysis and recalculating. Values are normalized to the North American Shale Composite (NASC) of Condie (1993). **a** Si and Al. **b** K and Na. **c** Mg and F. **d** Zr, Ti, and Nb

section. There is, however, a distinct low in Ca within the clay boundary layer at the top of Unit 2 (Fig. 5).

Salient features of the siliciclastic geochemistry of the measured section, i.e., with the carbonate and phosphate components removed, are given in Fig. 9. First, although the Al content of the siliciclastic fraction is approximately the same as the North American Shale Composite (NASC; Condie 1993), the Si content is only about 85–90% of the NASC. Conversely, while K is similar to NASC, Na is 3–5 times higher, a feature also noted in other Newark Supergroup sediments (van de Kamp and Leake 1996). Cogent stratigraphic variations in the siliciclastic component include an F spike in the insect layer (J1), a drop in both Mg and F, exclusive of that bound in phosphate, which coincides with the boundary between Units 2 and 3, and a spike in Zr, Nb, and Ti that coincides with the sand layer (Fig. 9c, d). While Ti and Nb values are consistent with average shale values, Zr (except in the sand layer) is depleted by a factor of 5.

Dolomite chemistry

In most of the measured section, zoned dolomite has Ca-rich cores and Fe- and Mn-rich rims (Fig. 10a–c). Mg in dolomite decreases at the boundary between Units 2 and 3 (Fig. 9c). The core and rim values for dolomite tend to covary within the section. The overall range in dolomite composition is small, with an average near $Ca_{55}Mg_{38}Fe_7$ (Fig. 10d). Nevertheless, the observed compositional range is well outside the range of analytical error (Fig. 10e).

Discussion

Origin of the dolomite and evidence for salinity/alkalinity

Recent research documents that primary precipitation of dolomite is mostly biomediated within lacustrine systems (Wright 1999; Calvo et al. 2003; Gierlowski-Kordesch 2010). In modern lakes, dolomite precipitation occurs in Mg- and Ca-rich waters with elevated salinity, alkalinity (pH > 8) and Mg/Ca ratios (>10), and low dissolved sulfate (DeDeckker and Last 1989). In such situations, tiny sub-micron-size crystals often characterize the dolomitic sediments (DeDeckker and Last 1989), which is reminiscent of the micro- to pseudosparry dolomite seen in the insect layer. The presence of carbonaceous, wavy clay units coupled with the dolomite layers suggests that the dolomite phase may be biologically mediated (Fig. 4f). The source of Ca and Mg could be the nearby Paleozoic

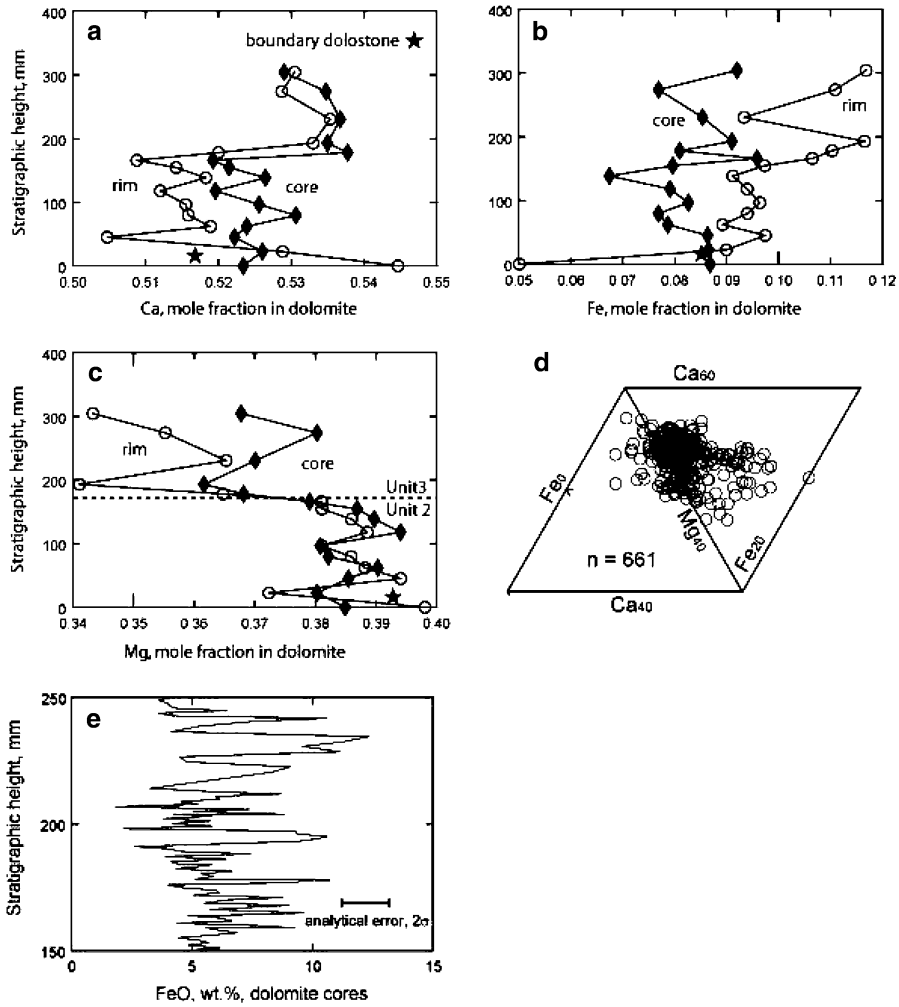

Fig. 10 Stratigraphy vs. dolomite chemistry. **a** Ca. **b** Fe. **c** Mg. **d** Mg–Ca–Fe (molar), all dolomite spot analyses. **a**–**c** all plot the cores and rims of zoned crystals averaged over the interval of the defined blocks. Dolomite grains in transition layer (*star*) were too small to clearly resolve core vs. rim. **e** Variation in Fe content of dolomite, by electron microprobe, over 100 mm of the measured section. FeO in individual analyses ranges from <3 to >12 wt%. These variations far exceed analytical error

limestones (north/northwest of the site) discussed by Watson and Grasty (1915). Thus, dolomite precipitation at Solite is likely biomediated in Mg- and Ca-rich saline and alkaline waters.

The coarsening of and development of zoning in dolomite crystals in the Solite sediments is almost certainly diagenetic. However, several observations suggest that dolomite is also a primary phase in the Solite measured section. First, the size of the microsparry dolomite crystals in the Solite sediments (5–20 μm) falls within the range of biologically mediated, primary dolomite, 1–120 μm (Gierlowski-Kordesch 2010). Second, there is striking variability in the modal abundance of dolomite on a sub-millimeter scale (Figs. 4e, 5, 7a). In fact, the laminae bear a marked resemblance to interlayered dolomite- and clay-rich laminae reported from several modern lakes in which dolomite is being precipitated—compare Fig. 4e with Last and DeDeckker (1990), as well as the Jurassic Hartford Basin (Gierlowski-Kordesch and Rust 1994) and the Eocene Green River Formation in Wyoming (Eugster and Hardie 1975). Lastly, high porosity and permeability are often needed for secondary dolomite precipitation. However, the lithologies here are mostly mudrocks and have low values for both porosity and permeability, and further suggest that the dolomite is primary.

Dolomite in the measured section is also chemically variable, on both coarse and fine scales. For example, dolomite in Unit 2 is typically more Mg-rich than that in Unit 3 (Fig. 10c). FeO variation in cores of dolomite crystals far exceeds analytical error (Fig. 10e). This is difficult to explain by

wholesale, late diagenetic dolomitization of the section, although recrystallization is possible if chemical re-distribution is limited. The dolomite core compositions, as well as the microspar, probably reflect bulk chemistry that existed in the sediment at and/or just after the time of deposition.

Presence of oxygen

If total organic carbon (TOC) is taken as a first order measure of oxygenation, then the measured section becomes less oxygenated towards the top (Fig. 5a). This interpretation is supported by up-section increases in S, P, and transition metals, decreases in TOC/S ratios, and color changes in the clay size fraction from brown in Unit 2 to black in Unit 3 (Figs. 4, 5, 8). By these measures, the insect layer appears to reflect the most oxygen-rich depositional environment in the measured section, while the fish layer appears the least oxygenated. Ca/Mn ratios suggest oxygenation for the measured section lies near the dysoxic/anoxic boundary, consistent with TOC content.

Depositional environments

Rate of deposition

The measured section lies within the penultimate Van Houten cycle in Quarry B (Olsen et al. 1989; Fig. 2). These cycles, deposited over a period of approximately 20,000 years (Olsen 1986), are approximately 10 m thick, for an average deposition rate of about 0.5 mm/year. This accumulation rate is similar to rates observed in Australian dolomite lakes (5 m/10,000 years; Gell et al. 1994). If one assumes that this is the maximum rate of deposition for the lake sediments, the measured 332 mm section represents a minimum of 650 years.

Silty claystone in Unit 1 (Block J2)

We interpret Unit 1 to be a freshwater marsh or swamp deposit, with abundant microbial carbon input, similar to the interpretation of other organic-rich mudstone and claystone units in nearby rift basins (Gore 1986; Olsen et al. 1991). This would account for its relatively high TOC and S contents relative to the overlying insect beds, its lack of aquatic vertebrate fossils, and its relatively poor lamination. In freshwater marshy environments fringing saline lakes in Australia and East Africa, organic-rich silts and clays are often poorly laminated (Coshell and Rosen 1994; Deocampo 2002). The fact that the silty claystone is then capped by the overlying dolostone suggests a post-depositional change in water chemistry that led to the precipitation of the boundary dolostone.

Boundary dolostone

This unit is unique and provides a sharp demarcation between the largely siliciclastic, fossil-poor siltstones of Unit 1 and the dolomite-rich sediments of the insect layer above. Its deposition reflects an abrupt, and within the context of the measured section, permanent chemical and/or physical transition. The top of the boundary dolostone appears to be a depositional hiatus, with small intraclasts in the base of the overlying insect layer.

The cracking and local perforation of the unit may reflect compaction, syneresis, or desiccation. The up-curled edges that characterize desiccation cracks are lacking, but the cracks are small (2–3 mm long, 0.5 mm wide), always wedge downwards, and where the layer is broken entirely apart, the edges are deformed and wide gaps develop, features more common in desiccation than syneresis cracks. Although sedimentary dikes, soft-sediment folds, and other indications of seismic mobilization of sediments are common in the Solite Quarry, these features are not found in association with the boundary dolostone. The cracking is strictly limited to the dolomite layer itself. Syneresis typically does not produce multiple cracks that originate along the same horizon; instead, cracks that are constrained to a single horizon are more indicative of desiccation and/or compaction (Collinson and Thompson 1982; Pratt 1998). Furthermore, Demicco and Hardie (1994) suggest that syneresis does not occur in carbonate sediments at all. Evidence of erosion at the top of the boundary dolostone, e.g., intraclasts in the overlying sediment, weakens the argument that these may be compaction cracks. The material filling the cracks consists of silicate material that is distinctly different from the surrounding, and especially, the overlying sediment (Fig. 4d). In fact, the material infilling the cracks extends above the edge of the boundary

dolostone into the overlying layer, suggesting that these cracks once extended higher than they do now. If we interpret the top of the boundary dolostone as a hiatus, it stands to reason that the curled edges of desiccation cracks may once have existed, but have since been eroded away and are now represented by rare intraclasts in the immediately overlying insect layer.

Algal carbonate mats are found at the edges of modern alkaline dolomitic lakes (DeDeckker 1988). While the boundary dolostone lacks the wavy, irregular lamination characteristic of algal carbonate mats (Tucker and Wright 1990), we interpret this unit as a microbially-mediated, primary dolomite deposit that reflects a sudden increase in the alkalinity and/or salinity of the lake margin. It is likely that the boundary dolomite layer formed from a lake margin seep. Seeps are common on the margins of lakes and can provide the appropriate dissolved ions necessary to precipitate carbonates (Scholl 1960; Cohen and Thouin 1987; Barrat et al. 2000; Pache et al. 2001). In this case, dissolution of the nearby Paleozoic limestones to the north/northwest could provide the necessary Mg and Ca ions (Watson and Grasty 1915). While the dolostone unit is thin (<3 mm), it is laterally extensive and can be traced up to 200 m across the quarry. The units above the boundary dolostone indicate a lake transgression, and the activity of the seep may have been triggered by a shift in climate towards more humid conditions thereby increasing hydraulic head to the seep ("forced convective flow", see Duffy and Al-Hassan 1988). The dolostone contains less organic carbon towards the top, perhaps reflecting a decrease in productivity accompanying the environmental change or a change in preservation potential.

Insect layer (J1) and Unit 2

The insect layer and the overlying beds of Unit 2 represent permanent lake deposits. The permanency of the lake is indicated by: (1) no evidence of desiccation, i.e., no soil horizons, mudcracks, or hiatuses, (2) the presence of aquatic reptiles and insects, and (3) carbonate laminites. The lack of evidence for exposure and/or evaporite precipitation, along with the preservation of lamination, suggests that the depositional environment was consistently inundated and quiet. Furthermore, the geochemical and sedimentologic analyses of the insect layer imply that the permanent lake responsible for the insect layer was saline and alkaline and that the depositional environment was shallow. Both freshwater and salt lake systems can produce primary dolomite, but shallow, saline, alkaline, high Mg/Ca ratio systems are most conducive (Last 1990). Similar interpretations (shallow, littoral) have been inferred for other ancient dolomite-producing basins (Valero Garces and Gisbert Aguilar 1994; Gierlowski-Kordesch and Rust 1994), and further work on lacustrine carbonate sediments that preserve lamination, e.g., carbonate laminites, suggest that the depositional environment can be shallow (littoral to sublittoral) to profundal, but that deep-water conditions are not necessary to preserve lamination (Last 1990; Gierlowski-Kordesch and Rust 1994; Larsen et al. 1998; Last et al. 1998; Carroll and Bohacs 1999; Finkelstein et al. 1999; Gierlowski-Kordesch 2010). Gierlowski-Kordesch and Rust (1994) discuss alternating carbonate-siliciclastic mudrocks with irregular lamination from the Hartford Basin that resemble the laminites discussed here. They report that these types of sediments are similar to those found in modern, shallow, saline lakes in Australia, forming in only a few meters of water (Last and DeDeckker 1990). Other basins within the Newark Supergroup, e.g. Newark Basin, also exhibit these microsparry laminites (de Wet et al. 2002).

The fossil biota in the insect layer also suggest a shallow, nearshore environment. Terrestrial insects are found entombed in some modern lake sediments, almost exclusively in a nearshore setting (DeDeckker 1988). Aquatic insects, particularly belostomatids (the most common insect type at Solite), also favor shallow waters close to shore (Hilsenhoff 1991). While the amphibious reptile *Tanytrachelos* is abundant in the insect layer, fish remains, including coprolites, are exceptionally rare. As one moves upsection in Unit 2 above the insect layer, fish, and especially coprolites, become more common. Larger fishes, including the palaeoniscoid, *Turseodus*, and the coelacanth, *Pariostegus*, appear.

Although the insect layer is very restricted in thickness, there are subtle differences in the distribution of the insects within the layer, both laterally and vertically. Belostomatid water bugs are the predominant group, with more than 2,000 specimens in the collections, and the total number of

belostomatids exceeds the totals of all others insect groups combined. The water bugs include all size classes, but numbers of nymphs are significantly greater than those of adults. The water bugs mostly occur in the lower third of the insect layer, with particularly high concentrations within the lower 2 mm of the unit. However, there is also some lateral variation and rarely, water bug numbers drop off dramatically so that they approach or even fall below the numbers of beetles. Occurrences of what Olsen et al. (1978; Fig 4a) identified as phyllocarids tend to closely match the water bug distribution. Their identity remains inconclusive, but we tend to support Shcherbakov's (2008) interpretation that these are dipteran pupae. This supports the interpretation that these insects were deposited in a shallow, inundated (littoral?) environment rather than a deep, anoxic profundal setting.

The terrestrial insect groups, such as dipterans, staphylinid beetles and archescytinids (terrestrial hemipterans) are distributed more or less uniformly throughout the thickness of the unit. Consequently, as numbers of truly aquatic insects diminish upwards, relative numbers of terrestrial insects increase toward the top of the insect layer. We suggest that this distribution of insects is entirely consistent with a transgressing sequence in which the aquatic forms concentrated near the base of the unit are suggestive of a very shallow lake margin environment. The more terrestrial forms are small flying insects that would have been wafted off shore by breezes. It is difficult to gauge the speed of the transgression, but obvious ripples and/or cross-bedding are absent and there are no indications of shoaling or discrete concentrations of the insects. While there is intermittent variation in the constitution or profile of the insect assemblage, over the entire width of the exposure (>400 m) the occurrence of insect fossils remains constant. Today, many insects are known to tolerate shorelines of modern alkaline and saline rift lakes in East Africa. Although they tend to be most abundant near sites of freshwater or hydrothermal springs (Scott et al. 2007, 2009), this is not exclusively so.

It seems reasonable to assume that the lack of bioturbation and the exquisite preservation of soft tissue are related, though it may seem contradictory to suggest that the insect layer is the most oxygenated of the sediments studied and yet exhibits no bioturbation. In fact, not only do the sediments lack burrows, but despite evidence for a well established or even luxuriant terrestrial flora, there are no roots or other indications of aquatic plants. Both aquatic plants and burrows are common in modern shallow lakes, and in the marine record, sediments having carbon contents in the range of the insect layer, 1.5–2.0% TOC, are almost invariably bioturbated (Calvert et al. 1996). However, this was likely an alkaline (and possibly saline) lacustrine environment. In such environments, few plants and organisms can survive. In modern analogs, such as Pilot Valley, NV, only water bugs and saltgrass colonize the shore of highly saline, alkaline springs (Liutkus and Wright 2008). Furthermore, mainly salt-tolerant plants such as *Scirpus*, *Cyperus*, *Typha*, and insects, e.g., brine flies, can tolerate the shores of saline, alkaline rift lakes in East Africa (Renaut and Tiercelin 1994; Ashley et al. 2004; Scott et al. 2007, 2009). All life stages of water bugs are present in the Solite sediments, but because they breathe air, they were unlikely to have been affected by the water chemistry as long as a food source such as algae or other insects was available. Other aquatic organisms, both benthic and pelagic, as well as plants would not have been able to withstand such a harsh environment. High salinity has been cited as the reason for an absence of bioturbation in other Mesozoic rift basins in the US (Gierlowski-Kordesch and Rust 1994) and this, coupled with high alkalinity, is a likely reason for the lack of bioturbation in the insect layer. The seep responsible for the boundary dolostone layer was likely still active beneath the submerged lake margin, and could have provided a dense bottom layer of toxic water that precluded burrowing and plant colonization.

Therefore, the presence of lamination and the absence of bioturbation and predators need not be explained by significant water depth. Instead, the water chemistry needed to form dolomite laminites is enough to: (1) exclude biota, including plants, burrowers, terrestrial and aquatic organisms, (2) produce and conserve the lamination, and (3) provide an environment conducive to insect preservation. Furthermore, the insect layer has the highest fluorine concentration of any unit in the measured section, a concentration several times higher than typical shales (Fig. 9c), and may be a result of re-circulated fluids coming up through the lake margin seep. The F in the

insect layer is not bound in phosphate (Fig. 7f) and reflects high F in the water column rather than F scavenged during the formation of diagenetic apatite. There are many F-rich deposits in rift basin systems throughout the world (see Van Alstine 1976) as well as modern high fluorine rift lakes in East Africa (Kilham and Hecky 1973; Kilham and Cloke 1990; Gikunju et al. 1992). Additionally, recent work by Partey et al. (2009) documents barite-fluorine deposits in the Rio Grande Rift. In lakes where the F concentration is highest, the growth of aquatic plants like papyrus is inhibited and certain plant and animal groups such as copepods and diatoms do not occur (Kilham and Hecky 1973). The high F and barite content in the Solite sediments may, once again, reflect syndepositional circulation of alkaline brines within the rift valley system via a subaqueous seep, as is noted in other Newark Supergroup systems (van de Kamp and Leake 1996; El Tabakh and Schreiber 1998), and may have rendered the lake water and/or bottom sediments inhabitable for those organisms that receive their nutrients directly from the water column and/or sediments. While we have no evidence for cool or hydrothermal springs proper at this time, we cannot exclude the possibility that brines could re-circulate along underlying faults and affect the lake and lake-margin water chemistry, which is common in many rift systems. Additionally, while a source of the fluorine has not yet been confirmed in the bedrock surrounding the Solite Quarry, significant barite deposits are located in the region and could explain the high Ba and S levels (Watson and Grasty 1915).

Although the interpretation of dark, fine-grained laminated sediments in rift basin systems is most often attributed to a deep, anoxic setting, the data presented here better agree with an inference for a shallow saline, alkaline lake. For example, it is hard to imagine delicate insects descending through a significant water column without falling prey to the aquatic vertebrates that were present. Furthermore, the exquisite preservation of these articulated insects, complete with antennae and wings, negates a free-fall through a significant water body, as turbulence and subsequent disarticulation would likely occur. The inhospitable chemistry of the water excluded fish, aquatic plants, and infaunal organisms and was sufficient to produce the dolomitic laminae that make the insect layer sediments so distinct.

Fish layer (D2) and Unit 3

These appear to be the deepest lake deposits in the measured section. Not only are these the least oxygenated sediments, as noted by high TOC and high S content, but fossils of large fish are common. The lake had to have been productive enough to support predatory fish because coprolites and gastric ejecta produced by large fish-eating vertebrates are common and contribute greatly to the high concentrations of P in parts of Unit 3. Graded sand and silt beds are probably turbidites and indicate subaqueous gravity transport of sediment. The presence of fish in a lake system implies that the lake is connected to a stable, long-lived fluvial system.

Diagenesis

The siliciclastic fraction in the measured section is strongly enriched in Na and depleted in Zr and Si relative to the NASC (Fig. 9). Strong Na-enrichment, including the formation of authigenic analcime, has been observed in several Newark Supergroup sedimentary sequences (van de Kamp and Leake 1996; El Tabakh and Schreiber 1998). Values of 4–7 wt% Na_2O have been measured in lacustrine mudstones in the Newark, Hartford, and Deerfield Basins, leading van de Kamp and Leake (1996) to conclude that up to 4 wt% Na_2O had been diagenetically added to the sediment. Mineralogic studies in the Newark Basin have supported this conclusion (El Tabakh and Schreiber 1998), suggesting that circulation of brines during lake lowstands was largely responsible for the addition of Na. Na_2O in the Solite measured section ranges from 4.4 to 6.2 wt% on a carbonate-free basis. This is within the range reported from shales elsewhere in the Newark Supergroup and a similar diagenetic origin for the excess Na in the Solite measured section seems likely (van de Kamp and Leake 1996).

One of the striking features of the measured section is the near total absence of quartz in the coarse, sand and silt siliciclastic fraction, and the presence of albite, which was confirmed by petrography and X-ray diffraction. Given that quartz is abundant in local source rocks and a common constituent of sandstones and conglomerates in the Danville Basin in general, we regard the absence of quartz as a diagenetic feature. The reaction,

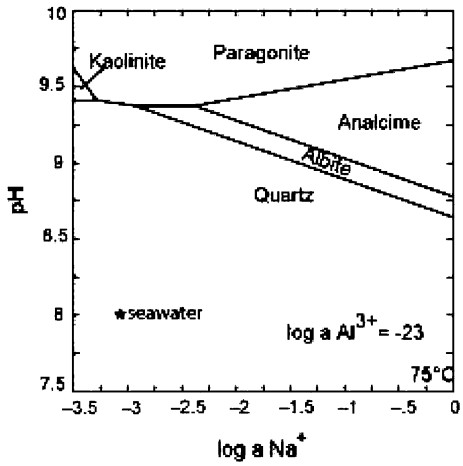

Fig. 11 Quartz and albite stability as a function of pH and Na activity. Quartz is unstable at elevated pH. Quartz stability also decreases with increasing temperature

clay + quartz + Na = albite or analcime, was postulated by van de Kamp and Leake (1996) to explain the low abundance of quartz in albite-rich lake beds. This quartz-consuming reaction is favored by high pH (Fig. 11, drawn after The Geochemists Workbench, v. 6.0; Bethke 2005). Recent work (Ayers and Zhang 2005) has shown that zircon is strongly susceptible to dissolution in alkaline environments. The depletion of Zr in the measured section, relative to both the NASC and to other High Field Strength Elements (HFSE) (Fig. 9d), further supports our conclusion that the fluids that affected the measured section were alkaline.

Paleogeography

The Solite Quarry sediments were deposited in a near-equatorial rift basin in the interior of the Pangaean supercontinent (Olsen and Johansson 1994). The abundance of plants and large animals, even dinosaurs, indicated that this was an environment with enough precipitation to support sizable biomass. Conversely, the sensitivity of the depositional environment to relatively minor changes in solar radiation, represented by Van Houten cycles, suggests that this was likely a balanced-fill lake system, in which potential accommodation was approximately equal to the sediment and water input (Carroll and Bohacs 1999).

We follow Olsen et al. (1978) in interpreting the Solite Quarry's measured section as rift valley lake deposits. Sedimentologic and geochemical characteristics imply that the sediments above the boundary dolostone were deposited in a permanent, saline, and alkaline lake. Although the water column in the paleo-lake may have supported abundant life, the sediment and bottom waters did not, as noted by the lack of bioturbation. This has been observed in modern lakes and is usually related to stratification of the water column and lack of oxygen in the bottom sediments of deep lakes (Buatois and Mangano 2008). Here, we suggest that the boundary dolostone indicates a lake margin seep that likely provided alkaline waters (high Mg, Ca, and F) that precluded infaunal plant and insect colonization.

Following the lake model of Carroll and Bohacs (1999), the deposits at the Solite Quarry appear to represent the fluctuating profundal facies associations of a balanced-fill lake system, matching the facies association model in stratal pattern, lithology, structure, biota, and organic matter. This interpretation best explains much of the measured section, in particular the fish layer and much of Unit 3. However, it would be highly speculative to extrapolate a 334 mm section to the basin scale.

The chemical, biotic, and sedimentologic features suggest that the insect layer was deposited in shallow water during a period of lake lowstand and initial transgression. First, the insect layer immediately overlies a hiatus above the boundary dolostone that exhibits possible desiccation features. Second, unlike sediments higher in the measured section, the chemistry of the insect layer sediment does not indicate anoxia and instead points to a shallow, saline alkaline environment suitable for laminite production. Finally, although large coprolites and fossils of large fish are common in Unit 3, they are exceptionally rare in the insect layer, much rarer, for example, than fossils of the aquatic reptile *Tanytrachelos*. All of these observations are consistent with a shallow, rather than deep, lake depositional environment for the insect layer sediments.

Freshwater deposits (Unit 1) give way up-section to shallow (the insect layer) and, later, to deeper, permanent, alkaline lake deposits (Units 2 and 3). This accounts for the presence of fish throughout much of the measured section, the near-shore/shallow water character of the insect layer sediments, and the anoxic character of the sediments with the most abundant fish. Therefore, we interpret the measured section as the record of a transgressive expansion of

an established rift lake. The major transition in the section, represented by the boundary dolostone, is interpreted as initial flooding of the lakeshore by saline and alkaline water from a lake margin seep during a rise of a rift valley lake.

While the sediments of this measured section fall within Division 2 of Van Houten cycle 2 in the Solite Quarry, it is important to remember that they represent only 650 years of accumulation. Thus, the disparity between sediments that preserve desiccation and a subsequent transgression within Division 2 sediments, which represent a high lake stand, is reconcilable if one considers that short-term climate change and basin dynamics such as tectonics and sediment supply, can occur (a) without cyclicity and (b) on much shorter time scales than orbital changes. Therefore, these sediments likely represent a short event, <1,000 years, which may have occurred independent of the overarching modulating climate cycles. Alternatively, the dichotomy between the Division connotation and the sedimentologic interpretation may indicate that the boundary between Division 1 and Division 2 sediments in this section at the Solite Quarry has been inaccurately identified and includes Division 1 sediments, indicative of shallow conditions, in the overlying Division 2 units.

Conclusions

The insect layer was deposited in shallow water during the initial transgression of a long-lived, saline alkaline, rift valley lake. The spectacular preservation of soft tissue in the insect layer reflects a paucity of predators and bioturbation that is attributed to saline and alkaline water chemistry that was necessary to produce the dolomitic laminites seen within the sediments. It is also possible that sediment/water toxicity (alkaline, high F) from seep brines inhibited bioturbation and predation as well. Although the initial conditions of preservation may be remarkable, it is perhaps equally remarkable that the fossils survived diagenesis that included dissolution of quartz and substantial coarsening of dolomite.

This work is among the first attempts to apply detailed geochemical/stratigraphic analysis to the study of *Lagerstätten*. For *Lagerstätten* of limited stratigraphic extent, such as the insect layer, our approach was successful in constraining aspects of the depositional and diagenetic history of the *Lagerstätte*, providing, for example, strong evidence for a shallow-water depositional environment and permitting detailed analysis of changing conditions prior to, during, and after deposition of the *Lagerstätte*. This study documents a rapid environmental transition. Such transitions, especially transgressions, may provide conditions especially conducive to preservation and suggest a tool to be used in the search for other *Lagerstätten*.

Acknowledgments Thanks to Paul Olsen, Hans Sues, Dave Grimaldi, Brian Axsmith, and Dennis Kent for many fruitful discussions on Newark Supergroup paleontology and stratigraphy. We thank Paul Olsen, Dennis Kent, Brian Axsmith, Dave Grimaldi, Vladimir Blagoderov, Bruce Cornet, Michael Engels, Tam Nguyen, Christa Hampton and Julian McCarthy for their assistance in the field. Additional thanks go to Elizabeth Gierlowski-Kordesch, Bob Demicco, Richard Abbott, Sarah Carmichael, Carol de Wet, Dan Deocampo, Fred Webb, Jr., Katelyn McGinnis, and the group from PaleoLunch for their insight into the carbonate geochemistry and thin-section analysis. Special thanks to the editorial staff of the *Journal of Paleolimnology* and several anonymous reviewers for helpful reviews of an earlier version of this manuscript. Research into the paleontology and sedimentology of the Solite Quarry has been supported by National Science Foundation grant EAR 0106309 to Nicholas Fraser and David Grimaldi. The fieldwork was supported by a National Geographic Society grant to NCF and by the Virginia Museum of Natural History.

References

Ackermann RV, Schlische RW, Patiño LC, Johnson LA (2003) A *Lagerstätte* of rift-related tectonic structures from the Solite Quarry, Dan River/Danville rift basin. In: Le-Tourneau PM, Olsen PE (eds) The Great Rift Valleys of Pangea. Columbia University Press, New York, pp 118–133

Algeo TJ, Maynard JB (2004) Trace-element behavior and redox facies in core shales of Upper Pennsylvanian Kansas-type cyclothems. Chem Geol 206:289–318

Anderson J, Anderson H, Fatti P, Sichel H (1996) The Triassic explosion (?): a statistical model for extrapolating biodiversity based on the terrestrial Molteno formation. Paleobiology 22:318–328

Ashley GM, Mworia JM, Muasya AM, Owens RB, Driese SG, Hover VC, Renaut RW, Goman MF, Mathai S, Blatt SH (2004) Sedimentation and recent history of a freshwater wetland in a semi-arid environment: Loboi Swamp, Kenya, East Africa. Sedimentology 51:1201–1321

Ayers JC, Zhang L (2005) Zircon aqueous solubility and partitioning systematics. Goldschmidt conference abstracts, Moscow, vol 15, p A5

Barrat JA, Boulègue J, Tiercelin J-J, Lesourd M (2000) Strontium isotopes and rare-earth element geochemistry

of hydrothermal carbonate deposits from Lake Tanganyika, East Africa. Geochim Cosmochim Acta 64:287–298
Berner RA, Raiswell R (1984) C/S method for distinguishing freshwater from marine sedimentary rocks. Geology 12:365–368
Bethke CM (2005) The Geochemists Workbench®, version 6.0, GWB essentials guide. Hydrogeology Program, University of Illinois, Urbana, 76 pp
Blagoderov V, Grimaldi DA, Fraser NC (2007) How time flies for flies: diverse Diptera from the Triassic of Virginia and early radiation of the order. Am Mus Novit 3572:1–39
Buatois LA, Mangano MG (2008) Applications of ichnology in lacustrine sequence stratigraphy: potential and limitations. Palaeogeogr Palaeoclimatol Palaeoecol. doi:10.1016/j.palaeo.2008.10.012
Calvert SE, Bustin RM, Ingall ED (1996) Influence of water column anoxia and sediment supply on the burial and preservation of organic carbon in marine shales. Geochim Cosmochim Acta 60:1577–1593
Calvo JP, McKenzie JA, Vasconcelos C (2003) Microbially-mediated lacustrine dolomite formation: evidence and current research trends. In: Valero-Garcés BL (ed) Limnogeology in Spain: a tribute to Kerry Kelts. Consejo Superior de Investigaciones Cientificas, Madrid, pp 229–251
Carroll AR, Bohacs KM (1999) Stratigraphic classification of ancient lakes: balancing tectonic and climatic controls. Geology 27:99–102
Cohen AS, Thouin C (1987) Nearshore carbonate deposits of Lake Tanganyika. Geology 15:414–418
Collinson JD, Thompson DB (1982) Sedimentary structures. George Allen and Unwin, London
Condie KC (1993) Chemical composition and evolution of the upper continental crust: contrasting results from surface samples and shales. Chem Geol 104:1–37
Coshell L, Rosen MR (1994) Stratigraphy and Holocene history of Lake Hayward, Swan Coastal Plain wetlands, western Australia. In: Renaut RW, Last WM (eds) Sedimentology and geochemistry of modern and ancient Saline Lakes. Special publication 50. SEPM, Tulsa, pp 173–188
de Wet CB, Mora CI, Gore PJW, Gierlowski-Kordesch E, Cucolo SJ (2002) Deposition and geochemistry of lacustrine and spring carbonates in Mesozoic rift basins, eastern North America. In: Renaut RW, Ashley GM (eds) Sedimentation in continental rifts. Special publication 73. SEPM, Tulsa, pp 309–325
DeDeckker P (1988) Biological and sedimentary facies of Australian salt lakes. Palaeogeogr Palaeoclimatol Palaeoecol 62:237–270
DeDeckker P, Last WM (1989) Modern, non-marine dolomite in evaporitic playas of western Victoria, Australia. Sediment Geol 64:223–238
Demicco RV, Hardie LA (1994) Sedimentary structures and early diagenetic features of shallow marine carbonate deposits. Atlas series 1. SEPM, Tulsa, 265 pp
Deocampo DM (2002) Sedimentary processes and lithofacies in lake-margin groundwater-fed wetlands in East Africa. In: Ashley GM, Renaut RW (eds) Sedimentation in continental rifts. Special publication 73. SEPM, Tulsa, pp 295–308
Duffy CJ, Al-Hassan S (1988) Groundwater circulation in a closed desert basin: topographic scaling and climate forcing. Water Resour Res 24:1675–1688
El Tabakh M, Schreiber BC (1998) Diagenesis of the Newark Rift Basin, eastern North America. Sedimentology 45:855–874
Eugster HP, Hardie LA (1975) Sedimentation in an ancient playa-lake complex: the Wilkins Peak Member of the Green River Formation of Wyoming. Geol Soc Am Bull 86:319–334
Finkelstein DB, Hay RL, Altaner SP (1999) Origin and diagenesis of lacustrine sediments, upper Oligocene Creede Formation, southwestern Colorado. Geol Soc Am Bull 111:1175–1191
Fraser NC, Grimaldi DA (2003) Late Triassic continental faunal change: new perspectives on Triassic insect diversity as revealed by a locality in the Danville basin, Virginia, Newark Supergroup. In: Letourneau PM, Olsen PE (eds) The Great Rift Valleys of Pangaea in Eastern North America: sedimentology, stratigraphy and paleontology, vol 2. Columbia University Press, New York, pp 192–205
Fraser NC, Grimaldi DA, Olsen PE, Axsmith B (1996) A Triassic *Lagerstätte* from eastern North America. Nature 380:615–619
Fürsich FT, Sha J, Jiang B, Pan Y (2007) High resolution palaeoecological and taphonomic analysis of Early Cretaceous lake biota, western Liaoning (NE-China). Palaeogeogr Palaeoclimatol Palaeoecol 253:434–457
Gall JC (1971) Faunes et paysages du Grès à Voltzia du Nord des Vosges. Essai Paléoécologique sur le Bundsandstein supérieur. Mémoires du Service de la Carte géologique d'Alsace-Lorraine 34:1–318
Gell PA, Barker PA, DeDeckker P, Last WM, Jelicic L (1994) The Holocene history of West Basin lake, Victoria, Australia; chemical changes based on fossil biota and sediment mineralogy. J Paleolimnol 12:235–258
Gierlowski-Kordesch E (2010) Lacustrine carbonates. In: Alonso-Zarza AM, Tanner LH (eds) Carbonates in continental settings, vol 61. Elsevier, Amsterdam, pp 1–101
Gierlowski-Kordesch E, Park LE (2004) Comparing species diversity in the modern and fossil record of lakes. J Geol 112:703–717
Gierlowski-Kordesch E, Rust BR (1994) The Jurassic East Berlin Formation, Hartford Basin, Newark Supergroup (Connecticut and Massachusetts): a saline lake-playa-alluvial plain system. In: Renaut RW, Last WM (eds) Sedimentology and geochemistry of modern and ancient Saline Lakes. Special publication 50. SEPM, Tulsa, pp 249–265
Gikunju JK, Maitho TE, Birkeland JM, Lökken P (1992) Fluoride levels in water and fish from Lake Magadi (Kenya). Hydrobiologia 234:123–127
Gore PJW (1986) Depositional framework of a Traissic rift basin: The Durham and Sanford sub-basins of the Deep River Basin, North Carolina. In Textoris DA (ed) Southeastern United States: Third Annual Midyear Meeting, Raleigh, North Carolina, Field Guidebook, SEPM, Field Trip no. 3, pp 55–115
Grimaldi D, Shmakov A, Fraser N (2004) Mesozoic thrips and early evolution of the order Thysanoptera (Insecta). J Paleontol 78:941–952
Grimaldi D, Junfeng Z, Fraser NC, Rasnitsyn A (2005) Revision of the bizarre Mesozoic scorpionflies in the

Pseudopolycentropodidae (Mecopteroidea). Insect Syst Evol 36:443–458
Heggie D, Skyring G (2005) Ozestuaries database. On line at www.ozestuaries.org/indicators/In_toc_ts_f.html. Maintained by Geosciences Australia
Hilsenhoff WL (1991) Diversity and classification of insects and collembolan. In: Thorp JH, Covich AP (eds) Ecology and classification of North American freshwater invertebrates. Academic Press, Inc., San Diego, pp 593–663
Horton JW, McConnell KJ (1991) The western piedmont. In: Horton JW, Zullo VA (eds) The geology of the carolinas. The University of Tennessee Press, Knoxville, pp 36–58
Kent DV, Olsen PE (1997) Paleomagnetism of Upper Triassic continental sedimentary rocks from the Dan River-Danville rift basin (eastern North America). Geol Soc Am Bull 109:366–377
Kilham P, Cloke PL (1990) The evolution of saline lake waters: gradual and rapid biogeochemical pathways in the Bosatu Lake District, Tanzania. Hydrobiologia 197:35–50
Kilham P, Hecky RE (1973) Fluoride: Geochemical and ecological significance in east African waters and sediments. Limnol Oceanogr 18:932–945
Larsen CPS, Pienitz R, Smol JP, Moser KA, Cumming BF, Blais JM, Macdonald GM, Hall RI (1998) Relations between lake morphometry and the presence of laminated lake sediments: a re-examination of Larsen and Macdonald (1993). Quat Sci Rev 17:711–717
Last WM (1990) Lacustrine dolomite; an overview of modern, Holocene, and Pleistocene occurrences. Earth Sci Rev 27:221–263
Last WM, DeDeckker P (1990) Modern and Holocene carbonate sedimentology of two saline volcanic maar lakes, southern Australia. Sedimentology 37:967–981
Last WM, Vance RE, Wilson S, Smol JP (1998) A multi-proxy limnologic record of rapid early Holocene hydrologic change on the northern Great Plains, southwestern Saskatchewan, Canada. Holocene 8:503–520
Leventhal JS (1995) Carbon-sulfur plots to show diagenetic and epigenetic sulfidization in sediments. Geochim Cosmochim Acta 59:1207–1211
Liutkus CM, Wright JD (2008) The influence of hydrology and climate on the isotope geochemistry of playa carbonates: a study from Pilot Valley, Nevada, USA. Sedimentology 55:965–978
Meyertons CT (1963) Triassic formations of the Danville basin. Virginia Division of Mineral Resources, Report of Investigations, vol 6, pp 1–65
Muttoni G, Kent DV, Olsen PE, Di Stefano P, Lowrie W, Bernasconi SM, Hernandez FM (2004) Tethyan magnetostratigraphy from Pizzo Mondello (Sicily) and correlation to the Late Triassic Newark astrochronological polarity time scale. Geol Soc Am Bull 116:1043–1058
Olsen PE (1979) A new aquatic eosuchian from the Newark Supergroup (Late Triassic-Early Jurassic) of North Carolina and Virginia. Postilla 176:1–14
Olsen PE (1986) A 40-million-year lake record of early Mesozoic orbital climatic forcing. Science 234:842–848
Olsen PE, Johansson AK (1994) Field guide to Late Triassic tetrapod sites in Virginia and North Carolina. In: Fraser NC, Sues H-D (eds) In the shadow of the dinosaurs. Cambridge University Press, New York, pp 408–443
Olsen PE, Remington CL, Cornet B, Thomson KS (1978) Cyclic change in Late Triassic terrestrial communities. Science 201:729–733
Olsen PE, Schlische RW, Gore PJW (1989) Tectonic, depositional, and paleoecological history of early Mesozoic Rift Basins, Eastern North America. 28th International geological congress, guidebook for field trip T351, American Geophysical Union, Washington, DC
Olsen PE, Froelich AJ, Daniels DL, Smoot JP, Gore PJW (1991) Rift basins of early Mesozoic age. In: Horton W (ed) Geology of the carolinas. University of Tennessee Press, Knoxville, pp 142–170
Pache M, Reitner J, Arp G (2001) Geochemical evidence for the formation of a large Miocene "travertine" mound at a sublacustrine spring in a soda lake (Wallerstein Castle Rock, Nördlinger Ries, Germany). Facies 45:211–230
Park LE, Downing KF (2001) Paleoecology of an exceptionally preserved arthropod fauna from lake deposits of the Miocene Barstow Formation, Southern California, USA. Palaios 16:175–184
Partey F, Lev S, Casey R, Widom E, Lueth VW, Rakovan J (2009) Source of fluorine and petrogenesis of the Rio Grande Rift-Type barite-fluorite-galena deposits. Econ Geol 104:505–520
Pratt BR (1998) Syneresis cracks: subaqueous shrinkage in argillaceous sediments caused by earthquake-induced dewatering. Sediment Geol 117:1–10
Quinby-Hunt MS, Wilde P (1996) Chemical depositional environments of calcic marine black shales. Econ Geol 91:4–13
Renaut RW, Tiercelin J-J (1994) Lake Bogoria, Kenya rift valley—a sedimentological overview. In: Renaut RW, Last WM (eds) Sedimentology and geochemistry of modern and ancient Saline Lakes. Special publication 50. SEPM, Tulsa, pp 101–123
Schlische RW (2003) Progress in understanding the structural geology, basin evolution, and tectonic history of the eastern North American rift system. In: LeTourneau PM, Olsen PE (eds) The Great Rift Valleys of Pangea in Eastern North America: tectonics, structure, and volcanism, vol 1. Columbia University Press, New York, pp 21–64
Scholl DW (1960) Pleistocene algal pinnacles at Searles Lake, California. J Sediment Petrol 30:414–431
Scott J, Renaut RW, Owen RB, Sarjeant WAS (2007) Biogenic activity, trace formation, and trace taphonomy in the marginal sediments of saline, alkaline Lake Bogoria, Kenya Rift Valley. In: Bromley RG, Buatois LA, Mangano G, Genise JF, Melchor RN (eds) Sediment-organism interactions; a multifaceted ichnology. Society for sedimentary geology special publication 88, pp 311–332
Scott J, Renaut RW, Buatois LA, Owen RB (2009) Biogenic structures in exhumed surfaces around saline lakes: an example from Lake Bogoria, Kenya Rift Valley. Palaeogeogr Palaeoclimatol Palaeoecol 272:176–198
Shcherbakov DE (2008) Insect recovery after the Permian/Triassic crisis. Alavesia 2:125–131
Tucker ME, Wright VP (1990) Carbonate sedimentology. Blackwell Scientific Publications, Oxford
Valero Garces BL, Gisbert Aguilar J (1994) Permian saline lakes in the Aragón-Béarn basin, western Pyrenees. In:

Renaut RW, Last WM (eds) Sedimentology and geochemistry of modern and ancient Saline Lakes. Special publication 50. SEPM, Tulsa, pp 267–290

Van Alstine RE (1976) Continetal rifts and lineaments associated with major fluorspar districts. Econ Geol 71:977–987

van de Kamp PC, Leake BE (1996) Petrology, geochemistry, and Na-metasomatism of Triassic-Jurassic non-marine clastic sediments in the Newark, Hartford, and Deerfield rift basins, northeastern USA. Chem Geol 133:89–124

Watson TL, Grasty JS (1915) Barite of the Appalachian states. Chem Eng 21:135–143

Wright VP (1999) The role of sulphate-reducing bacteria and cyanobacteria in dolomite formation in distal ephemeral lakes of the Coorong region, South Australia. Sediment Geol 126:147–157